The effect of pore structure on ebullition from peat

Jorge A. Ramirez[1,2] *, Andy J. Baird[1], Tom J. Coulthard[3]

[1]School of Geography, University of Leeds, Leeds, LS2 9JT, UK

[2]Department of Geosciences, Florida Atlantic University, Davie, Florida, 33314, USA

[3]Department of Geography, Environment, and Earth Sciences, University of Hull, Hull, HU6 7RX, UK

*Corresponding author (ramirez08063@alumni.itc.nl)

A paper for *Journal of Geophysical Research: Biogeosciences*

Key points:

Structural differences in peat determine if ebullition is steady or erratic and extreme

A physical model is capable of representing naturally occurring methane ebullition from peat

Bubble sizes from peat exhibit power law patterns

Abstract

The controls on methane (CH_4) bubbling (ebullition) from peatlands are uncertain, but evidence suggests that physical factors related to gas transport and storage within the peat matrix are important. Variability in peat pore size and the permeability of layers within peat can produce ebullition that ranges from steady to erratic in time, and can affect the degree to which CH_4 bubbles bypass consumption by methanotrophic bacteria and enter the atmosphere. Here we investigate the role of peat structure on ebullition in structurally different peats using a physical model that replicates bubble production using air injection

into peat. We find that the frequency distributions of number of ebullition events per time and the magnitude of bubble loss from the physical model were similar in shape to ebullition from peatlands and incubated peats. This indicates that the physical model could be a valid proxy for naturally occurring ebullition from peat. For the first time, data on bubble sizes from peat were collected to conceptualize ebullition, and we find that peat structure affects bubble sizes. Using a new method to measure peat macro structure, we collected evidence that supports the hypothesis that structural differences in peat determine if bubble release is steady or erratic and extreme. Collected pore size data suggests that erratic ebullition occurs when large amounts of gas stored at depth easily move through shallower layers of open peat. In contrast, steady ebullition occurs when dense shallower layers of peat regulate the flow of gas emitted from peat.

Index terms: 0428 (carbon cycling), 0497 (wetlands), 4468 (Nonlinear geophysics: Probability distributions, heavy and fat-tailed)

Key words: peatland, greenhouse gas, methane ebullition, pore structure

1. Introduction.

Methane (CH_4) is a powerful greenhouse gas that has a global warming potential 28 times that of carbon dioxide over a 100 year time-horizon [*Myhre et al.*, 2013]. A major, naturally-occurring, source of CH_4 is peatlands [*Blodau*, 2002; *Lai*, 2009], which consist of slowly decomposing plant and animal material that is mostly saturated with water. Transport mechanisms deliver CH_4 from the source of production within the peat, through the oxic zone above the water table, and into the atmosphere. Depending on the transport mechanism CH_4 residence time within the oxic zone can be long, with consequently high rates of CH_4

consumption by methanotrophs; transport can also be fast, and bypass consumption. Three mechanisms are responsible for transport of CH_4 through and from peat: diffusion through water- and gas- filled pores, plant-mediated transport, and ebullition. The first process, diffusion, occurs along a CH_4-concentration gradient from sites of CH_4 production to the peatland surface and thence to the atmosphere. Diffusion is a slow process, and if an oxic peat layer is present, between 55 and 90% of CH_4 can be consumed by oxidizing bacteria [*Fechner and Hemond*, 1992; *Whalen and Reeburgh*, 2000; *van Winden et al.*, 2012]. Plant-mediated transport occurs within the stems of plants that serve as gas conduits delivering CH_4 from the roots to the atmosphere. Thus, CH_4 transported via this method can entirely bypass consumption in the oxic peat layer, causing high rates of CH_4 emission [*Frenzel and Rudolph*, 1998; *Noyce et al.*, 2014]. Although plant-mediated transport is an effective mechanism of CH_4 transport, it is dependent on the position of the water table, which determines if roots can access CH_4 within the anoxic layer [*Waddington et al.*, 1996]. Ebullition refers to the transport of CH_4 as gas bubbles that form in peat pore water. Importantly, the speed at which CH_4 bubbles arrive at the peat water table and move through the unsaturated zone affects how much of their CH_4 is consumed by methanotrophs. Larger bubbles in porous media, such as peat, rise faster than smaller bubbles [*Corapcioglu et al.*, 2004] and ebullition events consisting of larger CH_4 bubbles are more likely to bypass consumption by methanotrophs. Likewise if bubbles are lost steadily then much of their CH_4 may be consumed, whereas if bubbles are lost episodically, the capacity of methanotrophs to consume CH_4 may be overwhelmed [*Coulthard et al.*, 2009]. For this reason, depending on the peatland, episodic ebullition events are thought to be important sources of CH_4 emissions from peat to the atmosphere and may be comparable to emissions via diffusion and plant-mediated transport [*Baird et al.*, 2004; *Glaser et al.*, 2004; *Stamp et al.*, 2013].

The factors that control whether ebullition is steady or episodic remain uncertain, but evidence suggests that physical processes related to gas storage and transport within the peat structure are important [*Comas et al.*, 2014; *Klapstein et al.*, 2014; *Chen and Slater*, 2015]. Methane bubbles in peat can accumulate behind existing bubbles lodged in pore necks [*Baird and Waldron*, 2003; *Strack et al.*, 2005; *Kellner et al.*, 2006], underneath woody layers, or below well-decomposed layers of peat [*Rosenberry et al.*, 2003; *Glaser et al.*, 2004]. In such situations, stored bubbles are released in pulses or bursts (i.e., cyclical or episodic ebullition), whilst for peats that do not trap bubbles, ebullition is steady and will be directly related to production. Aside from peat structure, the physical processes that affect CH_4 production, consumption and transport can also influence the location, timing and size of ebullition [*Tokida et al.*, 2009]. For example, episodic ebullition has been correlated with decreasing atmospheric pressure, which increases gas volume and bubble buoyancy, and 'forces' gas to the peat surface [*Tokida et al.*, 2007; *Comas et al.*, 2011]. Likewise, changes in the water table can control the release of bubbles stored within peat [*Strack and Waddington*, 2007; *Bon et al.*, 2014; *Chen and Slater*, 2015]. Although these environmental drivers affect the occurrence and magnitude of ebullition, it remains uncertain as to how much peat structure alone modulates bubble accumulation, movement, and release.

We devised a set of experiments to test whether a physical model of peat could replicate the frequency and magnitude of ebullition events measured in the field, and to test the hypothesis that structural differences in peat control the degree to which bubble release is steady or episodic. We compared ebullition from two structurally different peats and characterised the differences by measuring the properties of the larger pores in each peat type.

2. Methodology.

2.1 Ebullition experiments.

The ebullition experiments were performed using a physical model that was designed and constructed to hold a sample of peat (Figure 1a). In summary, operation of the physical model began by inserting a peat sample (see details below) into a cylindrical enclosure, sealing the enclosure and filling it with water. Next, precise amounts of air were delivered automatically from syringes to needles inserted in openings at the base of the enclosure. The needles produced bubbles that moved through the peat sample and became trapped within the peat pores. Eventually bubbles of various sizes were released from the peat and were captured by high definition video (Figure 1a, dashed area above peat). The bubbles then made their way to a cylindrical gas trap located at the top of the physical model. When the air entered the gas trap it lowered the water level by displacing a quantity of water that exited the instrument via a tube and a head-control device. A second video camera was positioned to record the gas trap and therefore record the volumetric rate of bubble release (Figure 1a).

By replicating ebullition in peat with a physical model we were able to record bubble sizes as well as rates of bubble loss, whereas all previous field [*Goodrich et al.*, 2011; *Comas and Wright*, 2012; *Stamp et al.*, 2013] and laboratory [*Kellner et al.*, 2006; *Green and Baird*, 2011; *Yu et al.*, 2014] investigations of ebullition have only recorded rates of bubble loss. Use of the physical model also made it possible to control external variables that can affect ebullition including temperature [*Waddington et al.*, 2009], sunlight [*Panikov et al.*, 2007], and atmospheric pressure [*Tokida et al.*, 2005]. Maintaining constant external variables allowed us to exclude these as being possible causes of ebullition events, allowing us to see how much peat structure alone affected ebullition. Critically, our approach allows production, the site of production and peat structure all to be isolated so that the importance of each can

be quantified. In our experiments we kept both the rate and location of bubble production constant. By doing this, we were able to further isolate the effect of peat structure on ebullition.

A sample of near-surface *Sphagnum magellanicum* Brid. peat and one of *Sphagnum pulchrum* (Lindb. ex Braithw.) Warnst. peat were collected from Cors Fochno, a raised bog in west Wales (4°1W' 52°30'N). The samples were in the early stages of decomposition, and these two moss species were selected because they produce strongly contrasting litter/peat types that are commonly found in the shallow layers of northern peatlands. Structurally, *Sphagnum magellanicum* tends to decay in such a way that the plant retains its shape until fairly advanced decomposition [*Kettridge and Binley*, 2011]. In contrast, the leaves of *Sphagnum pulchrum* become detached from the branches during the early stages of decomposition and the stems collapse, forming a relatively dense 'mush' of stems and loose leaves [*Kettridge and Binley*, 2011].

In the field, peat samples approximately 160 mm height and 160 mm diameter were cut out using the 'scissor method' reported by Green and Baird [2011, 2013] which minimises damage to the peat sample. Each sample was placed within a plastic container and transported to the laboratory where it was kept in cold storage (4°C). Prior to the experiment, each sample was removed from cold storage, excess water within the container was drained, and the upper growing surface (1-2 cm) was trimmed using scissors. To make further trimming easier, the sample was frozen overnight. After 24 hours the frozen sample was removed from the container and allowed to thaw slowly at ambient temperature within the laboratory. Freezing and thawing peat can cause changes in peat pore structure, but these changes occur naturally during the winter in northern peatlands. For this reason freezing and

thawing of the peat samples is unlikely to have introduced unnatural changes to the pore structure. Our method of freezing and thawing has also been used by studies that measure peat pore size at greater detail [*Kettridge and Binley*, 2008; *Quinton et al.*, 2009] and these studies did not report unusual changes in pore size. Once the outer layers of the peat sample were thawed, the sample was trimmed to the dimensions of a transparent acrylic tube (130 mm height, 130 mm diameter) with dimensions smaller than the bottom cylinder of the physical model (275 mm height, 150 mm diameter). The peat sample was carefully inserted into the acrylic tube and allowed to thaw completely in cold storage. Once complete, the acrylic tube containing peat serves as a self-contained module, and allows peat samples to be easily inserted and removed from the physical model without causing further damage to the peat structure (Figure 1a).

For each experiment with the different peat type (*S. magellanicum* and *S. pulchrum*) the physical model was filled with de-aired water that was prepared by boiling de-ionized water for 10 minutes which was then cooled in an airtight container. The use of de-aired water minimizes the amount of bubbles coming out of solution during the experiment. The de-aired water was dyed blue to improve the visual contrast between air and water. To ensure a high level of saturation, the physical model was filled slowly from its base at the rate of 2 cm hr^{-1}. The level of saturation in each sample was not measured, but we assumed it was high because we employed the wetting techniques of *Beckwith and Baird* [2001], and they recorded saturations between 90 and 95%. Sixteen 22-gauge, 7.5 cm-long, blunt-nose needles were inserted 4 cm into the base of the peat through openings sealed with septa (Figure 1a). The outer annular part of the peat sample was not used for air injection. Therefore we avoided injecting air into the part of the peat most likely to have a disturbed pore structure. Each needle was connected to a 10 mL syringe that was placed onto a syringe pump pre-

programmed to deliver from an individual syringe a quantity of 8 mL of air at a rate of 1 mL min^{-1}. A complete injection of air consisted of simultaneously injecting 16 syringes into the peat sample, and 10 injections or experimental runs were performed per peat type, so affording replication for each sample. Within the physical model changes in ambient atmospheric pressure were not controlled for, but each experimental run took place over a short period of time (< 10 min) during which atmospheric pressure changes would have been negligible.

A high definition video camera (Sony HDR-XR105E) recording at 50 frames per second filmed the bubbles exiting the surface of the peat sample to measure bubble sizes (Figure 1a). Bubble size in this experiment was defined as the area encompassed by the outline of a bubble when imaged in profile and in two dimensions. To highlight bubble outlines, the bubble machine was fitted with a uniform background consisting of a frosted sheet, and backlighting was provided by a 500-W halogen lamp. To measure the volumetric rate of bubble release from the peat, a second high definition video camera (Sony HDRSR10E) was positioned to record the change in water level within a cylindrical gas trap (Figure 1a). To improve contrast between air and water within the gas trap, backlighting was provided by a second halogen light.

Video was converted into images at the rate of 1 frame per second for bubble sizes. Sampling bubble sizes every 1 s meant that all bubbles exited the camera's field of view before the next measurement; therefore, bubbles were not double counted. Images were automatically processed using a Sobel edge detector script [*Gonzalez and Woods*, 2008] within the ImageJ image processing program [*Schneider et al.*, 2012] to identify individual bubbles emitted from the peat and extract each bubble's major-axis and minor-axis. The image analysis script

was able to measure multiple bubbles simultaneously exiting the peat and no data on bubble sizes was lost (no bubbles were missed). From the images it was not possible to determine the depth of the bubble and it was assumed that the unknown third axis of the bubble was equal to the major-axis. Using these dimensions, all bubbles were assumed to be oblate spheroids and their volume estimated accordingly. Bubbles with size < 0.0005 mL were micro bubbles that formed on the interior surface of the physical model, presumably by dissolved gas coming out of solution, and were not included in the analysis. Due to the main tank of the physical model being cylindrical, a considerable amount of distortion occurred if bubbles were recorded near the tank's left and right edge, and bubbles near these tank edges were not analysed.

Video of the volumetric rate of bubble release was sampled every 5 s. Image processing of bubble release was performed using a colour-thresholding technique based on image hue saturation and brightness [*Schneider et al.*, 2012]. This technique was used to select the image pixels within the gas trap consisting of water, and measure their total area. By measuring the change in water area, the area occupied by air could be calculated and converted into a volume using the dimensions of the gas trap. This volume of gas is equivalent to the total amount of gas from all bubbles entering the gas trap every 5 s. It was found that the minimum discernible amount of change in area was approximately 17 mm^2 (equivalent to a volume of 0.79 mL), and changes in area less than this amount were not analyzed.

An additional control experiment was carried out where the physical model contained no peat sample, but was otherwise operated in the same way as the experimental runs with peat. Ideally, a steady input of gas injected into the physical model without peat would produce a

near constant volumetric rate of bubble release. However, we found that the volumetric rate of bubble release from the control experiment showed some variation, and these deviations were likely caused by experimental and image-processing error. Two specific causes of variation in the volumetric rate of bubble release were the adhesion of bubbles to the needle ends and the reduction in bubble velocity as the bubbles interacted with the roof of the physical model. This error likely also exists in the bubble release from the physical model peat runs but was not removed from the bubble release data. Instead, the mean of the volumetric rate of bubble release from the empty physical model run was chosen as an uncertainty threshold. Volumetric rate of bubble release values collected in the physical model peat runs below this threshold were considered a product of error and caution was made when drawing conclusions about these release events. Volumetric rate of bubble release values above the threshold were more likely reliable releases of gas from the peat.

Patterns in bubble size and volumetric rate of release were extracted by producing histograms with bin sizes one-tenth of the data range. Candidate distributions similar to bubble emissions from peat field [*Goodrich et al.*, 2011; *Stamp et al.*, 2013] and laboratory studies [*Kellner et al.*, 2006; *Yu et al.*, 2014] were used to determine the best fitting distributions to the bubble release histograms. Histograms of bubble size were fitted with power law distributions. The absolute goodness of fit of the distribution was computed using the *F*-test for bubble sizes and chi-squared statistic for volumetric rate of release.

2.2 Estimating pore structure of peat.

To determine if structural differences in the peat affect ebullition, various methods were considered to describe the pore structure of the peat samples quantitatively. Bulk density and porosity [*Boelter*, 1969] can provide information on the peat sample as a whole, but do not

provide information about the location and size of pores. Therefore, these metrics were discounted because they do not help distinguish between peats that have similar overall porosities, but different pore size distributions and pore connectivity. To obtain this additional information studies have adopted methods including slicing and imaging peat sections [*Quinton et al.*, 2008], or imaging entire peat samples using x-ray computed tomography [*Rezanezhad et al.*, 2009; *Kettridge and Binley*, 2011; *Turberg et al.*, 2014]. Of the methods available, x-ray computed tomography is the least intrusive, and provides fine spatial resolution images of peat structure in two or three dimensions. However, as we did not have access to an x-ray scanner, we instead analysed cross sections of peat. Traditionally peat samples are prepared for slicing by removing the moisture from the peat with acetone, and impregnating the peat with resin [*Quinton et al.*, 2008]. This preparation can lead to complications that can cause shrinkage of the pore network or the peat sample can secrete wax and make it difficult to image the pore structure [*Quinton et al.*, 2009]. Therefore, this method was not used and another slicing method was developed.

After the physical model experiments, each peat sample within its module, was drained and placed in a freezer. Draining of peat is a process that naturally occurs in peatlands and more than likely did not introduce abnormal changes to the pore structure. To obtain slices from a sample, the sample was removed from the freezer and a 2 cm notch was made vertically along the full length of the sample at the location where the sample was facing forward in the physical model experiments (Figure 1b). Next, the sample was placed horizontally in a mitre box and a medium-cut hand saw (8 teeth per 25 mm) was used to saw four latitudinal sections of peat spaced 1 cm apart (Figure 1b). More slices were not obtained from the lower 4 cm of the sample because this portion of the sample was not injected with air during the physical model experiments due to the length of the inserted needles (Figure 1b). Additionally, in

order to account for the possibility that bubbles at the location of injection altered the pore structure, we have obtained our first peat slice 1 cm above the location of the needle ends. All peat slices were placed in the freezer until photographing took place.

Each slice was removed from the freezer and placed on a plastic board with clearly marked ground control points, cardinal directions, and rulers for scale. The peat slice was then thawed at ambient temperature and positioned underneath a digital camera (Canon PowerShot A650 IS, 12.1 mega pixels) that was perpendicularly mounted at a height of 29 cm. Each slice was repeatedly photographed and rotated 90 degrees until four photographs were obtained. Each slice was lit from above with ambient fluorescent lighting and obliquely from the east using a 500-W halogen lamp to produce shadows caused by topographic depressions in the peat. All photographs were taken at night to keep lighting constant over the entire photo session (i.e., to remove light-bleeding effects from daylight windows in the laboratory).

Inspection of the photographs revealed that shadows coinciding with pores could only be extracted from the northeast quadrant of each of the four photographs per peat slice (Figure 2). This was possibly due to the positioning of the halogen lamp. Therefore, for each slice it was decided to analyse only the northeast quadrant from each of the four photos resulting in four quadrants per slice. Each photo was cropped to the extent of the upper right quadrant and was imported into a geographical information system (GIS, ESRI ArcMap 9.3). Here the images were classified into 10 classes using a minimum Euclidean distance classification method (ISODATA) that is commonly used to perform unsupervised classification of remotely-sensed images [*Ball and Hall*, 1965]. This classification method assigns each image pixel (consisting of red, green, and blue values) to a cluster of pixels with similar RGB

values. Each of these clusters represents a class, and the darkest pixels in the peat images formed a single cluster/class that represented shadows/pores. The resulting classified raster images of the slice quadrants were re-classified from ten classes into two classes. The new classification scheme contained one class with all the classified pixels that corresponded to pores and a second class containing the remaining pixels that represented peat or micro-pores that were not detectable (Figure 2b). These classified images were converted into vector GIS format and the size of each pore was calculated as an area (mm^2).

3. Results.

Bubble size distributions from the *S. magellanicum* (*n* = 2972 bubbles) and *S. pulchrum* (*n* = 5615 bubbles) peat samples both displayed power law patterns with similar slopes (Figure 3a). Where the two peat samples differ is in the magnitude and frequency of bubble sizes. On average, the *S. pulchrum* sample produced smaller bubbles (avg. bubble size = 0.025 mL) than the *S. magellanicum* sample (avg. bubble size = 0.052 mL), a 108% increase in average bubble size. The size range, maximum to minimum, of the *S. pulchrum* sample's bubbles (0.0008-0.3429 mL) is smaller than that from the *S. magellanicum* sample (0.0008-0.5233 mL). The largest bubbles from the *S. magellanicum* sample were 1.5 times larger than the largest bubble produced by the *S. pulchrum* sample. The volumetric bubble-release data from *S. magellanicum* (*n* = 536 releases) and *S. pulchrum* (*n* = 534 releases) were fitted with positively-skewed distributions, with smaller bubble release events occurring frequently and larger events rarely (Figure 3b). The best fitting distribution to *S. magellanicum* release was a gamma distribution (χ^2 = 6.4, p = 0.6) and to *S. pulchrum* a log-normal distribution (χ^2 = 15.1, p=0.06). The bubble release from the physical model run without peat was normally distributed (χ^2 = 9.0, p = 0.3), with a mean bubble release of 1.5 mL $5s^{-1}$, and this value was set as the uncertainty threshold (red line in Figure 3b). Overall release from *S. magellanicum*

($\bar{x}$ = 2.30 mL $5s^{-1}$, σ = 1.14 mL $5s^{-1}$) is greater and more frequent than events from *S. pulchrum* ($\bar{x}$ = 1.65 mL $5s^{-1}$, σ = 0.60 mL $5s^{-1}$). In Figure 3b it can be seen that both peat types have a similar probability of producing smaller release events, but a different probability of producing relatively larger release events occurring at the tail end of the distributions.

This difference in release is also visible when the release data are plotted as time series and 'extreme' bubble release events are isolated using the 90^{th} percentile of bubble release (3.23 mL) derived by combining the observations from both peat types (Figure 4). Clearly, *S. magellanicum* peat (Figure 4a) produces extreme release events more frequently than *S. pulchrum* peat (Figure 4b). Of the 349 release events recorded for *S. magellanicum*, 20% were extreme, and these extreme events comprised 36% of the total flux. In sharp contrast only 2% of the 446 releases from *S. pulchrum* were extreme, with 4% total flux being extreme. These larger, less frequent release events contribute to *S. magellanicum* peat (coefficient of variation (CV) = 49%) producing ebullition that is characteristically erratic when compared to the regularly occurring ebullition produced by *S. pulchrum* (CV = 36%). Furthermore, 72% of the bubble releases from *S. magellanicum* and 54% of the bubble releases from *S. pulchrum* were above the uncertainty threshold (red lines in Figure 4).

In Figure 5a the size and location of pores for each slice are visualized to determine if structural differences exist between the peat types and between the peat slices. Both peat types have pore sizes that are dominated by smaller pores (<10 mm^2) with relatively fewer large pores (>50 mm^2) (Figure 5b). The porosity of the peat types was calculated from the slices, but this porosity is an underestimate of true porosity because micro-pores (<0.004 mm^2) could not be detected. For this reason porosities are reported as detectable porosity. As

a whole, the two peat types do not differ in detectable porosity, with average detectable porosity of *S. magellanicum* and *S. pulchrum* being 23% and 22% respectively. Where the two peat types differ is the location of large and moderately sized pores at different peat depths. For example, the *S. magellanicum* peat slices S2, S3, S4 have similar porosities, with small to moderate pores occurring throughout (Figure 5a). This contrasts with the shallowest slice of *S. magellanicum* (Figure 5a, S1) peat which has a 9-10% increase in porosity and greater occurrence of large pores (Figure 5b, S1). Structural changes between peat slices of *S. pulchrum* are different from *S. magellanicum*. In *S. pulchrum* two layers of different detectable porosity can be distinguished between the combination of slices S3 and S4, and S1 and S2 (Figure 5a). The deeper peat layer (S3 and S4) has an open pore structure with large pores and the shallower peat layer (S1 and S2) has a closed structure dominated by smaller pores (Figure 5b).

4. Discussion.

This study has provided the first record of ebullition bubble sizes generated from peat in which the rate and location of gas bubble production is held constant. The bubble sizes from both peat types exhibit a power law pattern, and the second pattern produced by both peat types were positively skewed distributions for volumetric bubble release. These bubble-release patterns are similar to patterns found in observations of biogenic gas ebullition from peat [*Kellner et al.*, 2006; *Goodrich et al.*, 2011; *Stamp et al.*, 2013; *Yu et al.*, 2014]. The similarity in bubble release patterns from the physical model and the natural system suggests that peat structure may be a control on the pattern of bubble release in natural systems. A major advantage of the physical model is the possibility of controlling gas production, which helps isolate structural effects on ebullition from peat. Within our physical model, by controlling 'production' in two contrasting samples of peat we have been able to determine if

ebullition is a production-controlled process or whether storage and transport – in other words peat structure – are also important. Our results suggest that structure could be more important than production rate and location in controlling ebullition. However, applying our approach to more peat samples will be needed to test this interpretation.

It is possible to explain the differences in bubble release between the two peat types from the structural information obtained by slicing the peat. The pore sizes of the shallowest slices of peat (S1 and S2) may explain why *S. magellanicum* produces more extreme individual releases than *S. pulchrum*. From the pore-size information provided by Figure 5 the shallow slices of *S. magellanicum* contain large pores that can easily release gas stored in deeper slices and produce extreme, more erratic bubble releases. In contrast, shallow slices of *S. pulchrum* contain small pores, and, although *S. pulchrum* is able to store relatively large amounts of gas in its deeper slices (S3 and S4), the movement of gas through the shallower slices (S1 and S2) is partly hindered because passage through smaller pores requires greater amounts of buoyancy. These shallow slices of peat found in *S. pulchrum* effectively produce a 'seal' that may prevent the deeper gas from easily reaching the peat surface. In this experiment we do not have evidence that a less permeable peat layer or 'seal' will trap gas and rupture to produce extremely large bubble releases [*Glaser et al.*, 2004]. Instead, bubble escape from *S. pulchrum* suggests that less permeable layers of peat can impede gas movement, regulate ebullition, and give rise to smaller, more regularly occurring bubble releases in comparison to *S. magellanicm*.

Despite the novel data generated from these experiments, it remains difficult to explain the differences in bubble size between the two peat types. As bubbles move through the peat they change shape and size as they deform and conform to the geometry of the pores [*Corapcioglu*

et al., 2004]. When the bubbles emerge from the peat, it is possible that bubble size is related to the last pore a bubble has occupied. If we assume that this is occurring, the moderate to large pores existing in the shallow slice of *S. magellanicum* peat would produce more moderate to large bubbles (Figure 3a). This contrasts with the shallow slice from *S. pulchrum* which contains small pores, and would produce small bubbles emerging from the peat.

Studies using x-ray tomography have reported porosities from peat that range from 43-61% [*Quinton et al.*, 2009; *Rezanezhad et al.*, 2010], whilst the slicing method presented here found porosities between 17 and 30%. The difference in porosity between the two methods is most likely due to x-ray tomography producing images that are two times finer in spatial resolution than the digital images of the peat slices. This means that the peat slicing method is not suitable for imaging micro pores (<0.004 mm^2), but performs well when imaging larger pores. Furthermore, neither method is suitable for identifying exactly the pores in which gas is transported (effective porosity), but our physical model could be used to determine this property by injecting air into peat samples imaged within an X-ray computed tomography scanner. These images could be used to track the movement of gas within the peat matrix and calculate the effective porosity of the peat. This highlights a potential use for our physical model and an experiment that would be difficult to perform with peats containing natural production.

Until now we have not known whether signals of ebullition were simply a product of variations in gas production [*Coulthard et al.*, 2009], atmospheric pressure or whether the structure of the peat was also important. The results from this investigation confirm that peat structure can have an important role in regulating bubble size and release from peat. The patterns also show that peat structure alone can cause power law distributions of bubble sizes,

and positively skewed rates of bubble release. Moreover, changes in peat structure at different depths of peat can apparently determine if ebullition occurs erratically with extreme events, or more regularly. Overall, these findings suggest that it can not be assumed that two peat types with the same porosity must have the same bubble-release behaviour. Similarly it can not be assumed that large-pore porosities are a guarantee of similar ebullition behaviour.

One of the limitations of this experiment was the lack of replication as only one peat sample was obtained per peat type. Variability in pore structure within a peat type can occur and, as demonstrated here, these differences in pore structure may affect the magnitude and frequency of bubble sizes and release. It is possible that repeating this experiment with additional peat samples, of the same peat types, could produce the same patterns that were observed in bubble size (power law distribution) and release (non-normal, positively skewed distribution), but generate different magnitudes and frequencies for these patterns. For example, another sample of *S. pulchrum* may have a pore structure that results in significantly larger bubble sizes and release than observed from the sample used in this experiment. For this reason, throughout this investigation we refrain from making any conclusions that are specific to a peat type and focus on differences in bubbles size and release related to evidence obtained on pore structure. Future studies adopting our method of injecting gas into peat should contain multiple independent samples per peat type to statistically determine differences in ebullition between peat types.

5. Conclusions.

The recommendation for investigators of CH_4 emissions from peat is that peat structure should be accounted for when measuring and modelling ebullition from different peat types. Researchers measuring ebullition should consider that peat structure can produce

characteristically different ebullition that may be difficult to measure. Differences in peat structure could result in ebullition that is 'patchy' in space and erratic in time. We recommend that efforts be made to sample ebullition across structurally different peats to reduce uncertainty in CH_4 ebullition estimates. Models of ebullition in peat should not treat the peat profile as a single entity; those that do may not always be capable of representing ebullition properly [*Kellner et al.*, 2006]. Instead, models should explicitly represent the peat structure and account for gas dynamics including gas storage, accumulation, and release. Our magnitude and frequency distributions of bubble size could be used to guide model development and serve as an additional test for models that attempt to replicate ebullition from peat. Recent developments in modeling gas bubble dynamics with a reduced-complexity model [*Ramirez et al.*, 2015a, 2015b] provide a viable approach to simulating ebullition from peat, but more data are needed to test such models. This testing would require patterns of bubble size and release from a greater range of peat types with different pore structures. In our study we deliberately chose contrasting peat types, so our results may represent different ebullition behaviours. The challenge now is to investigate a range of peat types, and we recommend our experimental approach for doing such work. Consideration should also be given to allowing CH_4 to build up in peat samples naturally (and much more slowly) and recording the natural ebullition patterns through, for example, cameras that are triggered by ebullition events or time lapse cameras [*Comas and Wright*, 2012]. These natural ebullition patterns could also be compared against model simulations.

5. Acknowledgements.

This research was supported by a postgraduate fee waiver provided to JR by the School of Geography at the University of Leeds. Thanks are owed to Anthony Windross of the

University of Leeds for constructing the bubble machine. Contact the corresponding author (ramirez08063@alumni.itc.nl) for access to the data generated within this study.

6. References.

Baird, A. J., and S. Waldron (2003), Shallow horizontal groundwater flow in peatlands is reduced by bacteriogenic gas production, *Geophys. Res. Lett.*, *30*(20), doi:204310.1029/2003gl018233.

Baird, A. J., C. W. Beckwith, S. Waldron, and J. M. Waddington (2004), Ebullition of methane-containing gas bubbles from near-surface *Sphagnum* peat, *Geophys. Res. Lett.*, *31*(21), doi:L2150510.1029/2004gl021157.

Ball, G. H., and D. J. Hall (1965), *ISODATA, a novel method of data analysis and pattern classification*, DTIC Document.

Beckwith, C. W., and A. J. Baird (2001), Effect of biogenic gas bubbles on water flow through poorly decomposed blanket peat, *Water Resour. Res.*, *37*(3), 551–558.

Blodau, C. (2002), Carbon cycling in peatlands - A review of processes and controls, *Environ. Rev.*, *10*(2), 111–134, doi:10.1139/a02-004.

Boelter, D. H. (1969), Physical properties of peats as related to degree of decomposition, *Soil Sci. Soc. Am. Proc.*, *33*(4), 606–609, doi:10.2136/sssaj1969.03615995003300040033x.

Bon, C. E., A. S. Reeve, L. Slater, and X. Comas (2014), Using hydrologic measurements to investigate free-phase gas ebullition in a Maine peatland, USA, *Hydrol. Earth Syst. Sci.*, *18*(3), 953–965, doi:10.5194/hess-18-953-2014.

Chen, X., and L. Slater (2015), Gas bubble transport and emissions for shallow peat from a northern peatland: The role of pressure changes and peat structure, *Water Resour. Res.*, doi:10.1002/2014WR016268.

Comas, X., and W. Wright (2012), Heterogeneity of biogenic gas ebullition in subtropical peat soils is revealed using time-lapse cameras, *Water Resour. Res.*, *48*(4).

Comas, X., L. Slater, and A. S. Reeve (2011), Atmospheric pressure drives changes in the vertical distribution of biogenic free-phase gas in a northern peatland, *J. Geophys. Res.*, *116*(G4), G04014, doi:10.1029/2011jg001701.

Comas, X., N. Kettridge, A. Binley, L. Slater, A. Parsekian, A. J. Baird, M. Strack, and J. M. Waddington (2014), The effect of peat structure on the spatial distribution of biogenic gases within bogs, *Hydrol. Process.*, *28*(22), 5483–5494, doi:10.1002/hyp.10056.

Corapcioglu, M. Y., A. Cihan, and M. Drazenovic (2004), Rise velocity of an air bubble in porous media: Theoretical studies, *Water Resour. Res.*, *40*(4), 9, doi:W0421410.1029/2003wr002618.

Coulthard, T., A. J. Baird, J. Ramirez, and J. M. Waddington (2009), Modeling methane dynamics in peat: future prospects, in *Northern Peatlands and Carbon Cycling*, vol. 184, edited by A. J. Baird, L. R. Belyea, X. Comas, A. Reeve, and L. Slater, p. 299, American Geophysical Union, Washington D. C.

Fechner, E. J., and H. F. Hemond (1992), Methane transport and oxidation in the unsaturated zone of a *Sphagnum* peatland, *Global Biogeochem. Cycles*, *6*(1), 33–44,

doi:10.1029/91gb02989.

Frenzel, P., and J. Rudolph (1998), Methane emission from a wetland plant: the role of CH_4 oxidation in *Eriophorum*, *Plant Soil*, *202*(1), 27–32, doi:10.1023/a:1004348929219.

Glaser, P. H., J. P. Chanton, P. Morin, D. O. Rosenberry, D. I. Siegel, O. Ruud, L. I. Chasar, and A. S. Reeve (2004), Surface deformations as indicators of deep ebullition fluxes in a large northern peatland, *Global Biogeochem. Cycles*, *18*(1), GB1003, doi:10.1029/2003gb002069.

Gonzalez, R. C., and R. E. Woods (2008), *Digital Image Processing*, Prentice Hall, Upper Saddle River.

Goodrich, J. P., R. K. Varner, S. Frolking, B. N. Duncan, and P. M. Crill (2011), High-frequency measurements of methane ebullition over a growing season at a temperate peatland site, *Geophys. Res. Lett.*, *38*(7), L07404, doi:10.1029/2011gl046915.

Green, S. M., and A. J. Baird (2011), A mesocosm study of the role of the sedge *Eriophorum angustifolium* in the efflux of methane-including that due to episodic ebullition-from peatlands, *Plant Soil*, *351*(1-2), 207–218, doi:10.1007/s11104-011-0945-1.

Green, S. M., and A. J. Baird (2013), The importance of episodic ebullition methane losses from three peatland microhabitats: a controlled-environment study, *Eur. J. Soil Sci.*, *64*(1), 27–36, doi:10.1111/ejss.12015.

Kellner, E., A. J. Baird, M. Oosterwoud, K. Harrison, and J. M. Waddington (2006), Effect of temperature and atmospheric pressure on methane ebullition from near-surface peats, *Geophys. Res. Lett.*, *33*(18), doi:L1840510.1029/2006gl027509.

Kettridge, N., and A. Binley (2008), X-ray computed tomography of pent soils: Measuring gas content and peat structure, *Hydrol. Process.*, *22*(25), 4827–4837, doi:10.1002/hyp.7097.

Kettridge, N., and A. Binley (2011), Characterization of peat structure using X-ray computed tomography and its control on the ebullition of biogenic gas bubbles, *J. Geophys. Res.*, *116*(G1), G01024, doi:10.1029/2010jg001478.

Klapstein, S. J., M. R. Turetsky, A. D. McGuire, J. W. Harden, C. I. Czimczik, X. Xu, J. P. Chanton, and J. M. Waddington (2014), Controls on methane released through ebullition in peatlands affected by permafrost degradation, *J. Geophys. Res. Biogeosciences*, *119*(3), 418–431, doi:10.1002/2013JG002441.

Lai, D. Y. F. (2009), Methane dynamics in northern peatlands: a review, *Pedosphere*, *19*(4), 409–421.

Myhre, G., D. Shindell, F. Bréon, W. Collins, J. Fuglestvedt, J. Huang, D. Koch, J. Lamarque, D. Lee, and B. Mendoza (2013), Anthropogenic and natural radiative forcing Climate Change 2013: The Physical Science Basis. Contribution of Working Group I to the Fifth Assessment Report of the Intergovernmental Panel on Climate Change ed TF Stocker, D Qin, GK Plattner, M Tignor, SK Al,

Noyce, G. L., R. K. Varner, J. L. Bubier, and S. Frolking (2014), Effect of *Carex rostrata* on seasonal and interannual variability in peatland methane emissions, *J. Geophys. Res. Biogeosciences*, *119*(1), 24–34, doi:10.1002/2013JG002474.

Panikov, N. S., M. A. Mastepanov, and T. R. Christensen (2007), Membrane probe array: Technique development and observation of CO_2 and CH_4 diurnal oscillations in peat profile, *Soil Biol. Biochem.*, *39*(7), 1712–1723, doi:10.1016/j.soilbio.2007.01.034.

Quinton, W. L., M. Hayashi, and S. K. Carey (2008), Peat hydraulic conductivity in cold

regions and its relation to pore size and geometry, *Hydrol. Process.*, *22*(15), 2829–2837, doi:10.1002/hyp.7027.

Quinton, W. L., T. Elliot, J. S. Price, F. Rezanezhad, and R. Heck (2009), Measuring physical and hydraulic properties of peat from X-ray tomography, *Geoderma*, *153*(1-2), 269–277, doi:http://dx.doi.org/10.1016/j.geoderma.2009.08.010.

Ramirez, J. A., A. J. Baird, T. J. Coulthard, and J. M. Waddington (2015a), Ebullition of methane from peatlands: Does peat act as a signal shredder?, *Geophys. Res. Lett.*, *42*(9), 3371–3379, doi:10.1002/2015GL063469.

Ramirez, J. A., A. J. Baird, T. J. Coulthard, and J. M. Waddington (2015b), Testing a simple model of gas bubble dynamics in porous media, *Water Resour. Res.*, doi:10.1002/2014WR015898.

Rezanezhad, F., W. L. Quinton, J. S. Price, D. Elrick, T. R. Elliot, and R. J. Heck (2009), Examining the effect of pore size distribution and shape on flow through unsaturated peat using computed tomography, *Hydrol. Earth Syst. Sci.*, *13*(10), 1993–2002, doi:10.5194/hess-13-1993-2009.

Rezanezhad, F., W. L. Quinton, J. S. Price, T. R. Elliot, D. Elrick, and K. R. Shook (2010), Influence of pore size and geometry on peat unsaturated hydraulic conductivity computed from 3D computed tomography image analysis, *Hydrol. Process.*, *24*(21), 2983–2994, doi:10.1002/hyp.7709.

Rosenberry, D. O., P. H. Glaser, D. I. Siegel, and E. P. Weeks (2003), Use of hydraulic head to estimate volumetric gas content and ebullition flux in northern peatlands, *Water Resour. Res.*, *39*(3), doi:106610.1029/2002wr001377.

Schneider, C. A., W. S. Rasband, and K. W. Eliceiri (2012), NIH Image to ImageJ: 25 years of image analysis, *Nat. Methods*, *9*(7), 671–675.

Stamp, I., A. J. Baird, and C. M. Heppell (2013), The importance of ebullition as a mechanism of methane (CH_4) loss to the atmosphere in northern peatlands, *Geophys. Res. Lett.*, *40*(10), 2087–2090.

Strack, M., and J. M. Waddington (2007), Response of peatland carbon dioxide and methane fluxes to a water table drawdown experiment, *Global Biogeochem. Cycles*, *21*(1), doi:Gb100710.1029/2006gb002715.

Strack, M., E. Kellner, and J. M. Waddington (2005), Dynamics of biogenic gas bubbles in peat and their effects on peatland biogeochemistry, *Global Biogeochem. Cycles*, *19*(1), doi:Gb100310.1029/2004gb002330.

Tokida, T., T. Miyazaki, and M. Mizoguchi (2005), Ebullition of methane from peat with falling atmospheric pressure, *Geophys. Res. Lett.*, *32*(13), doi:10.1029/2005gl022949.

Tokida, T., T. Miyazaki, M. Mizoguchi, O. Nagata, F. Takakai, A. Kagemoto, and R. Hatano (2007), Falling atmospheric pressure as a trigger for methane ebullition from peatland, *Global Biogeochem. Cycles*, *21*(2), doi:10.1029/2006gb002790.

Tokida, T., T. Miyazaki, and M. Mizoguchi (2009), Physical controls on ebullition losses of methane from peatlands, in *Carbon Cycling in Northern Peatlands*, vol. 184, edited by A. J. Baird, L. R. Belyea, X. Comas, A. S. Reeve, and L. D. Slater, pp. 219–228, American Geophysical Union, Washington D. C.

Turberg, P., F. Zeimetz, Y. Grondin, C. Elandoy, and A. Buttler (2014), Characterization of structural disturbances in peats by X-ray CT-based density determinations, *Eur. J. Soil Sci.*, *65*(4), 613–624.

Waddington, J. M., N. T. Roulet, and R. V Swanson (1996), Water table control of methane emission enhancement by vascular plants in boreal peatlands, *J. Geophys. Res.*, *101*(D17), 22775–22785.

Waddington, J. M., K. Harrison, E. Kellner, and A. J. Baird (2009), Effect of atmospheric pressure and temperature on entrapped gas content in peat, *Hydrol. Process.*, *23*(20), 2970–2980, doi:10.1002/hyp.7412.

Whalen, S. C., and W. S. Reeburgh (2000), Methane oxidation, production, and emission at contrasting sites in a boreal bog, *Geomicrobiol. J.*, *17*(3), 237–251.

van Winden, J. F., G.-J. Reichart, N. P. McNamara, A. Benthien, and J. S. S. Damsté (2012), Temperature-induced increase in methane release from peat bogs: a mesocosm experiment, *PLoS One*, *7*(6), e39614.

Yu, Z., L. D. Slater, K. V. R. Schäfer, A. S. Reeve, and R. K. Varner (2014), Dynamics of methane ebullition from a peat monolith revealed from a dynamic flux chamber system, *J. Geophys. Res. Biogeosciences*, *119*(9), 1789–1806.

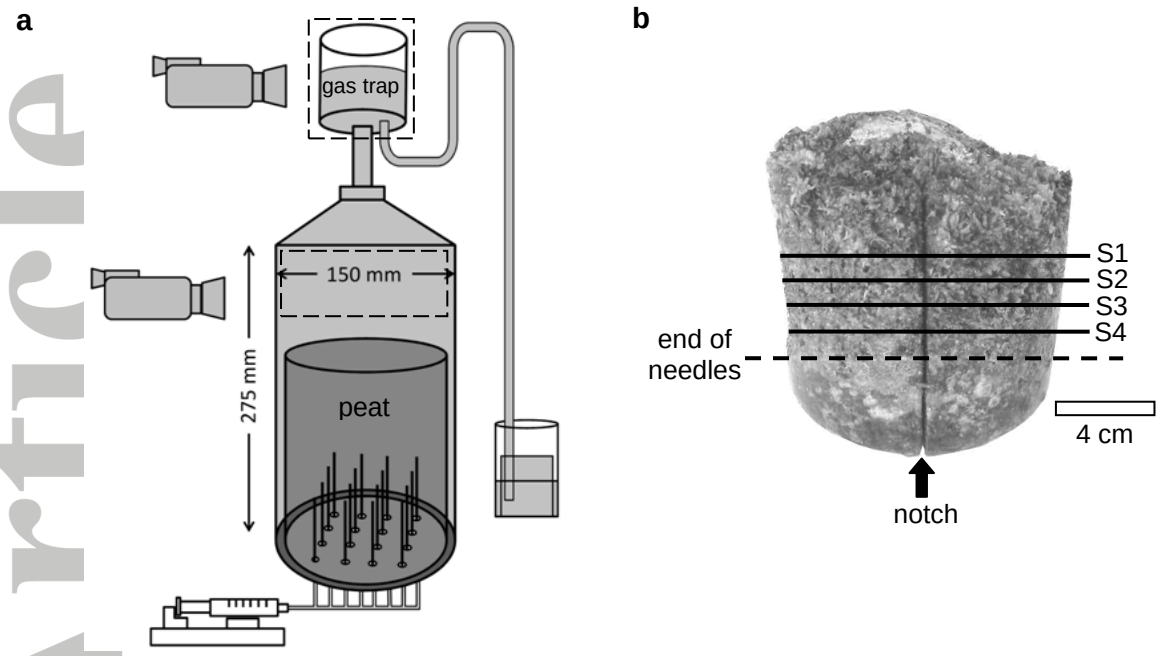

Figure 1. (a) Schematic of physical model of ebullition from peat with field of view of cameras filming bubble sizes and release. (b) Four slices at 1 cm intervals obtained from a peat sample. Dashed line marks approximate ends of the bubble-injection needles.

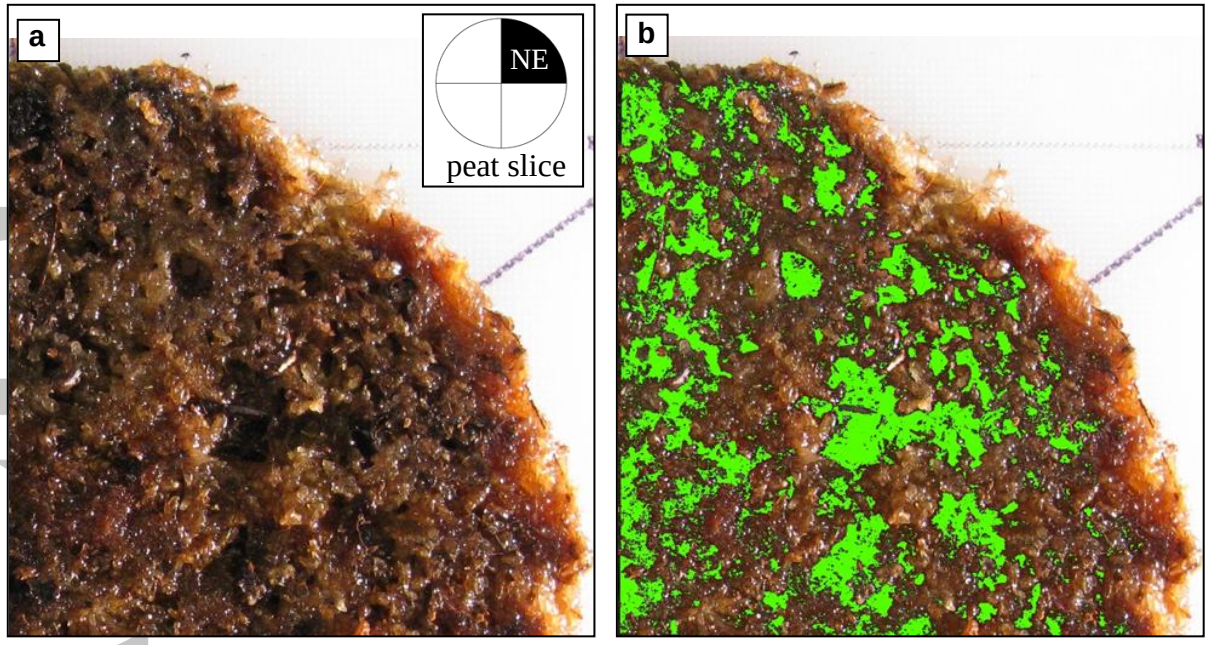

Figure 2. (a) Northeast quadrant of a peat slice of *S. magellanicum* peat with illumination from the east (b) Classified image of pore locations in green.

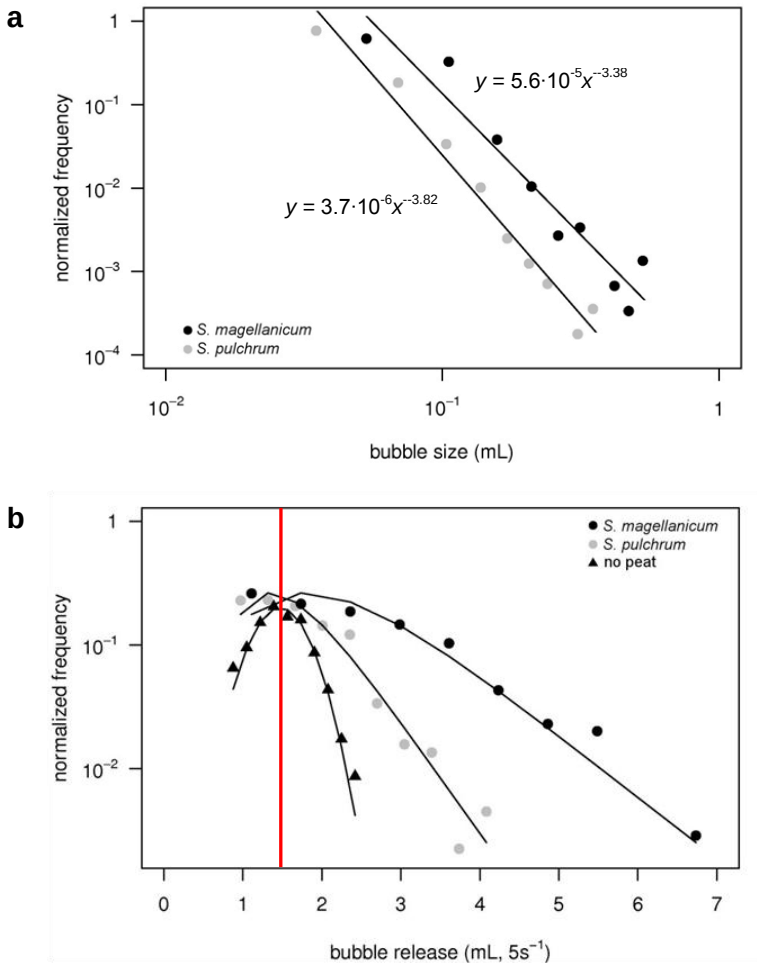

Figure 3. (a) Bubble size magnitude and frequency from *S. magellanicum* peat and *S. pulchrum* peat with fitted power law distributions having $p < 0.05$ and $r^2 > 0.92$. (b) Volumetric bubble release from *S. magellanicum* peat, *S. pulchrum* peat, and the physical model with no peat. The mean volumetric bubble release of the physical model run with no peat (1.5 mL $5s^{-1}$) represents the uncertainty threshold (red line).

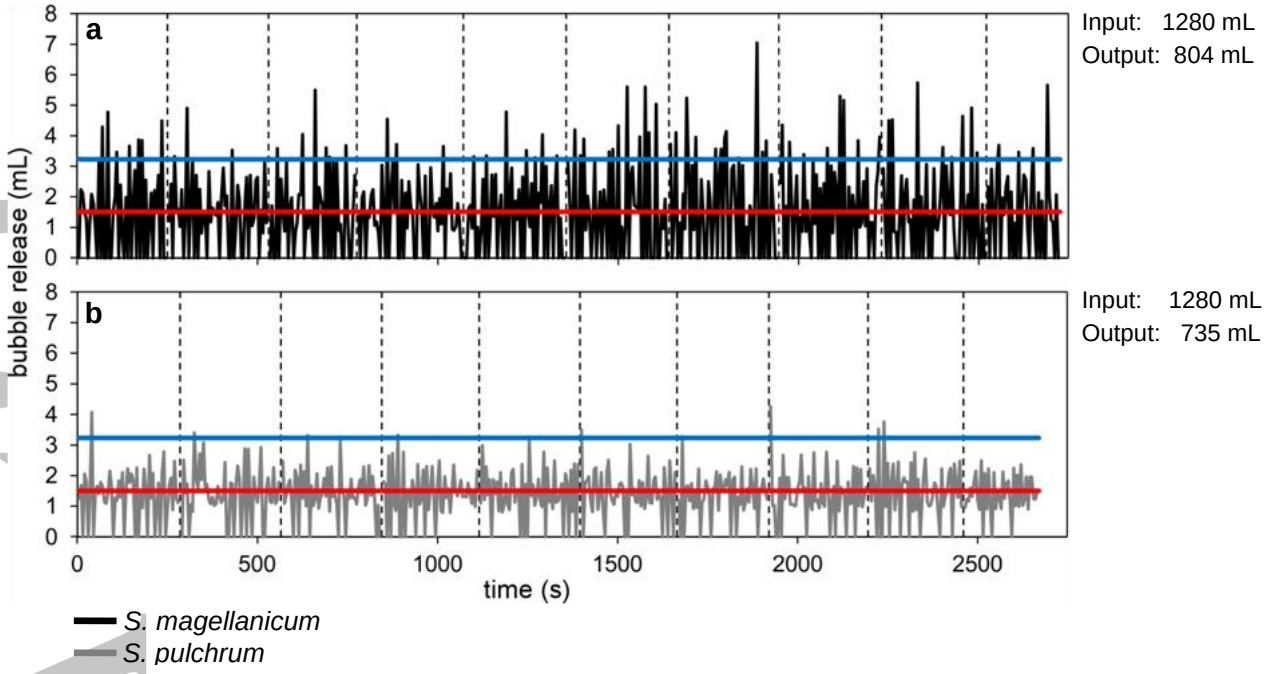

Figure 4. Time series of bubble release for (a) *S. magellanicum* peat and (b) *S. pulchrum* peat. Time series from 10 separate injections are plotted end-to-end for visualization purposes, and vertical dashed lines mark the end of each time series. The red line is the uncertainty threshold, and blue lines are 90th percentile of bubble release from both peat types.

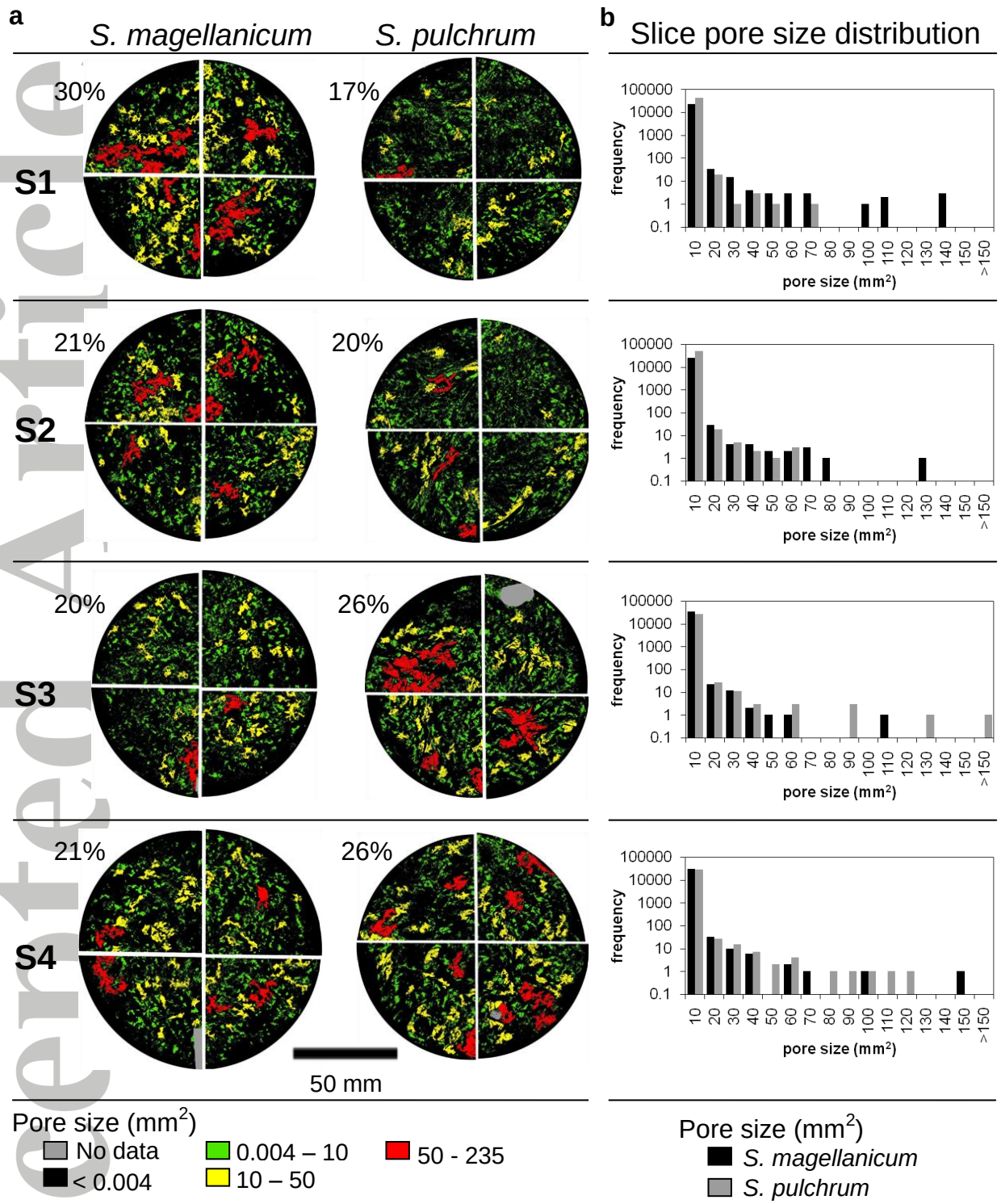

Figure 5. Mosaic and distribution of pore sizes.
(a) Analysed quadrant mosaiced to reconstruct slice pore size and location for *S. magellanicum* peat and *S. pulchrum* peat. Detectable porosity per slice is indicated. (b) Pore size distributions of each slice for each peat species.